Limnol. Oceanogr., 57(1), 2012, 1–17

doi:10.4319/lo.2012.57.1.0001

Carbon dynamics and community production in the Mississippi River plume

Xianghui Guo,[a,b] Wei-Jun Cai,[a,*] Wei-Jen Huang,[a] Yongchen Wang,[a] Feizhou Chen,[a] Michael C. Murrell,[c] Steven E. Lohrenz,[d] Li-Qing Jiang,[a,1] Minhan Dai,[b] Justin Hartmann,[a] Qi Lin,[e] and Randy Culp[f]

[a] Department of Marine Sciences, University of Georgia, Athens, Georgia
[b] State Key Laboratory of Marine Environmental Science, Xiamen University, Xiamen, P. R. China
[c] Gulf Ecology Division, U.S. Environmental Protection Agency, Gulf Breeze, Florida
[d] Department of Marine Science, University of Southern Mississippi, Stennis Space Center, Hancock County, Mississippi
[e] Key Laboratory of Global Change and Marine-Atmospheric Chemistry, Third Institute of Oceanography, State Oceanic Administration, Xiamen, P. R. China
[f] Center for Applied Isotope Study, University of Georgia, Athens, Georgia

Abstract

Dissolved inorganic carbon (DIC), total alkalinity (TAlk), pH, and dissolved oxygen (DO) were determined in the Mississippi River plume during five cruises conducted in the spring, summer, and fall. In contrast to many other large rivers, both DIC and TAlk were higher in river water than in seawater. Substantial losses of DIC, relative to TAlk, occurred within the plume, particularly at intermediate salinities. DIC removal was accompanied by high DO, high pH, and nutrient depletion, and was attributed to high phytoplankton production. As a result, the carbonate saturation in the plume became much higher than in ocean and river waters. A mixing model was used to determine DIC removal. We provide evidence that the use of a two–end-member (river and ocean) mixing model was valid during late summer and fall (low discharge period). However, for other periods we used salinity and TAlk to delineate a mixing model that included two river end members and an ocean end member. Net community production rates in the plume, estimated using a box model, peaked in the summer and were among the highest reported to date for large river plumes. In the summer and fall, biological production in the river plume consumed a majority of the available nutrients, whereas during the spring only a small fraction of the available nutrients were consumed in the plume. Biological production was the dominant process influencing pH and carbonate saturation state along the river–ocean gradient, whereas physicochemical dynamics of mixing played an important role in controlling the TAlk and DIC distributions of this large river plume.

Rivers and estuaries play an important role in the global carbon cycle, exporting $\sim 1 \times 10^{15}$ g C yr^{-1} to the oceans, of which 40% is dissolved inorganic carbon (DIC; Degens et al. 1991). It remains uncertain how these fluxes are regulated in coastal oceans and whether the latter act as a net source or sink for atmospheric carbon dioxide (CO_2; Smith and Hollibaugh 1993; Chen and Borges 2009; Cai 2011). In general, CO_2 release or uptake in coastal waters reflects a balance between respiration of riverine organic carbon (OC) and net in situ autotrophic production of OC in the surface mixed layer. However, physical transport and physicochemical dynamics of mixing can also play an important role. The net metabolic status of the coastal ocean is a topic that has been hotly debated (Smith and Hollibaugh 1993; Chen and Borges 2009; Cai 2011). The nature of this metabolic balance is particularly important in large river-dominated margins that are characterized by high carbon and nutrient inputs, which stimulate both primary production and microbial respiration with great spatial and seasonal variations. The mechanisms influencing net uptake and release of CO_2 in large river plume environments remain poorly understood because of limited research, the very different time scales for nutrient uptake (hours–days) and OC production and decomposition (days to weeks or longer), and the sensitive and nonlinear dependence of the carbonate system parameters along the river–ocean mixing gradient.

High productivity stimulated by river-borne nutrients has been observed in large river plumes, including the Amazon, Changjiang, and Mississippi Rivers (Lohrenz et al. 1997; Ternon et al. 2000; Chou et al. 2009*a*). Autotrophic activity depletes DIC, which can create an intensive but localized sink for atmospheric CO_2, such as that observed in the Changjiang plume and East China Sea shelf (Chou et al. 2009*a*; Zhai and Dai, 2009), the Amazon River plume and western tropical Atlantic Ocean (Ternon et al. 2000; Cooley and Yager 2006), and the Mississippi River plume (Cai 2003; Lohrenz et al. 2010). It is also expected that river plumes and their associated biogeochemical processes will greatly affect pH and carbonate saturation state (Salisbury et al. 2008; Borges and Gypens 2010). Nevertheless, our understanding of the role of inorganic carbon in contributing to coastal carbon budgets is still rather rudimentary.

The carbon cycle of the northern Gulf of Mexico is strongly affected by the Mississippi–Atchafalaya river system, which delivers 21×10^{12} g C yr^{-1} of DIC (Cai and Lohrenz 2010), 1.2–3.8 $\times 10^{12}$ g C yr^{-1} of particulate OC (Trefry et al. 1994; Duan and Bianchi 2006), 1.8–3.1 $\times$

* Corresponding author: wcai@uga.edu

[1] Present address: NOAA National Oceanographic Data Center, Silver Spring, Maryland

10^{12} g C yr^{-1} of dissolved OC (DOC) (Bianchi et al. 2004; Cai and Lohrenz 2010), and 1.0×10^{12} g N yr^{-1} of dissolved inorganic nitrogen (DIN) (Lehrter et al. 2009). How these carbon pools are being altered and at what rates are difficult to evaluate, as various studies have reported highly variable conditions, making it difficult to generalize source and sink terms of the carbon cycle. Based on a limited dataset and a simple two–end-member mixing scenario, a previous study of CO_2 dynamics in the Mississippi River plume estimated biological DIC uptake of 2–3 g C m^{-2} d^{-1} in August–September 1998 (Cai 2003). However, spatial distributions of partial pressure of CO_2 (pCO_2) and CO_2 flux in the Mississippi River plume were shown to be highly variable in June 2003 (Lohrenz and Cai 2006), and it will be shown here that a two–end-member mixing model rarely holds for the Mississippi River plume. Green et al. (2006) estimated the contribution of the river plume to the air–sea CO_2 flux based on an OC model. However, the net metabolic balance and the net carbon budget for the entire river plume remain largely unquantified, especially in the case of estimates based on field observations. Such field observations with adequate spatial and temporal coverage are a useful means to evaluate and refine existing (Green et al. 2006) and future models of the region.

Ocean acidification, the result of ocean uptake of atmospheric CO_2, has increased steadily over the past few decades, and has become a topic of global interest (Orr et al. 2005; Borges and Gypens 2010). It is debated whether the net effect of large rivers is to raise or lower coastal ocean pH (Salisbury et al. 2008; Borges and Gypens 2010). Based on a two–end-member mixing model, Salisbury et al. (2008) suggested that rivers decreased coastal ocean pH and carbonate saturation state, and thus negatively affect shell formation by calcareous organisms. Alternatively, a recent modeling study in Belgian coastal waters suggested that increased biological production due to increasing nutrient supply would increase coastal surface-water pH and carbonate saturation state (Borges and Gypens 2010). Similarly, recent reports from the Changjiang River plume showed that pH was high because of strong biological production in the plume (Chou et al. 2009*a*). These conflicting observations highlight the need for more study of these properties in large river systems.

In this study, we present the distributions of DIC, total alkalinity (TAlk), pH, and dissolved oxygen (DO) from five cruises in the surface mixed layer of the Mississippi River plume. Major biological and physical processes that control the carbonate properties are identified. Moreover, using carbonate system parameters in conjunction with a box model, net community production (NCP) within the spatial and temporal domains of the surface plume is quantified. We hypothesize that the Mississippi River plume is not well modeled as a two–end-member mixing system; instead, a three–end-member mixing model should be applied to the quasi-conservative carbonate parameter (e.g., TAlk) during most seasons. In addition, we hypothesize that the pH and carbonate saturation state of the plume are largely controlled by biological production rather than physicochemical dynamics of mixing. Because of the inherent complexity and large size of the system, we have limited our discussion to the plume and surrounding surface waters, but note that the metabolic state and carbonate chemistry in the subsurface and benthic systems underneath and downstream of the plume will exhibit different properties and merit further consideration in subsequent studies.

Methods

Site description—The Mississippi–Atchafalaya river system is the largest in North America, with annual loads of 580 km^3 of freshwater and 210×10^9 kg of sediment exported into the northern Gulf of Mexico (Milliman and Meade 1983). It drains 41% of the conterminous United States, and contributes over 90% of the freshwater to the Louisiana continental shelf (Dinnel and Wiseman 1986). River control structures direct 70% of the freshwater discharge directly onto the continental shelf through the Bird-foot Delta, with the remaining 30% passing through the shallow Atchafalaya Bay (Fig. 1A). Of the three major outflows in the Bird-foot Delta, Southwest Pass is the largest, accounting for $\sim$ 50% of the total (Hitchcock et al. 1997).

About 40–50% of the freshwater discharge of the Mississippi River flows westward onto the Louisiana–Texas continental shelf (Dinnel and Wiseman 1986), forming a stratified coastal current known as the Louisiana Coastal Current (Wiseman et al. 1997). The size and shape of the plume is strongly affected by seasonal wind and current patterns. Persistent southeast winds over the region set up a western flow over the shelf through most of the year (Cochrane and Kelly 1986), except in summer, when the coastal current becomes eastward (Ohlmann and Niiler 2005); the reversal usually starts around May or June (Cochrane and Kelly 1986). Large-scale circulation patterns often retain the freshwater on the shelf although the river flow is reduced in summer.

This study focused on the portion of the Louisiana continental shelf west of the Mississippi River and east of the Atchafalaya River, a region that is strongly affected by the Mississippi River and occasionally by outflow from the Atchafalaya River (Fig. 1A).

Field programs—Data were collected during five cruises on board the R/V *Pelican* and the Ocean Survey Vessel (OSV) *Bold*. These cruises covered spring (April 2006), summer (June 2006 and August 2004), and fall (September 2006 and October 2005). The October 2005 cruise was conducted about 1 month after Hurricane Katrina and 2 weeks after Hurricane Rita. The sampling stations are shown in Fig. 1B–F.

Surface-water samples were collected with 10-liter Niskin bottles (R/V *Pelican*) or 10-liter Go-Flo bottles (OSV *Bold*) mounted on a rosette sampler fitted with a Seabird® SBE 911 conductivity–temperature–depth sensor package. Samples for DO, pH, and DIC were taken with Tygon® tubing free of air bubbles and overflowed thoroughly. DO samples were collected into 60- or 300-mL biochemical oxygen demand bottles and fixed with Winkler reagents. pH

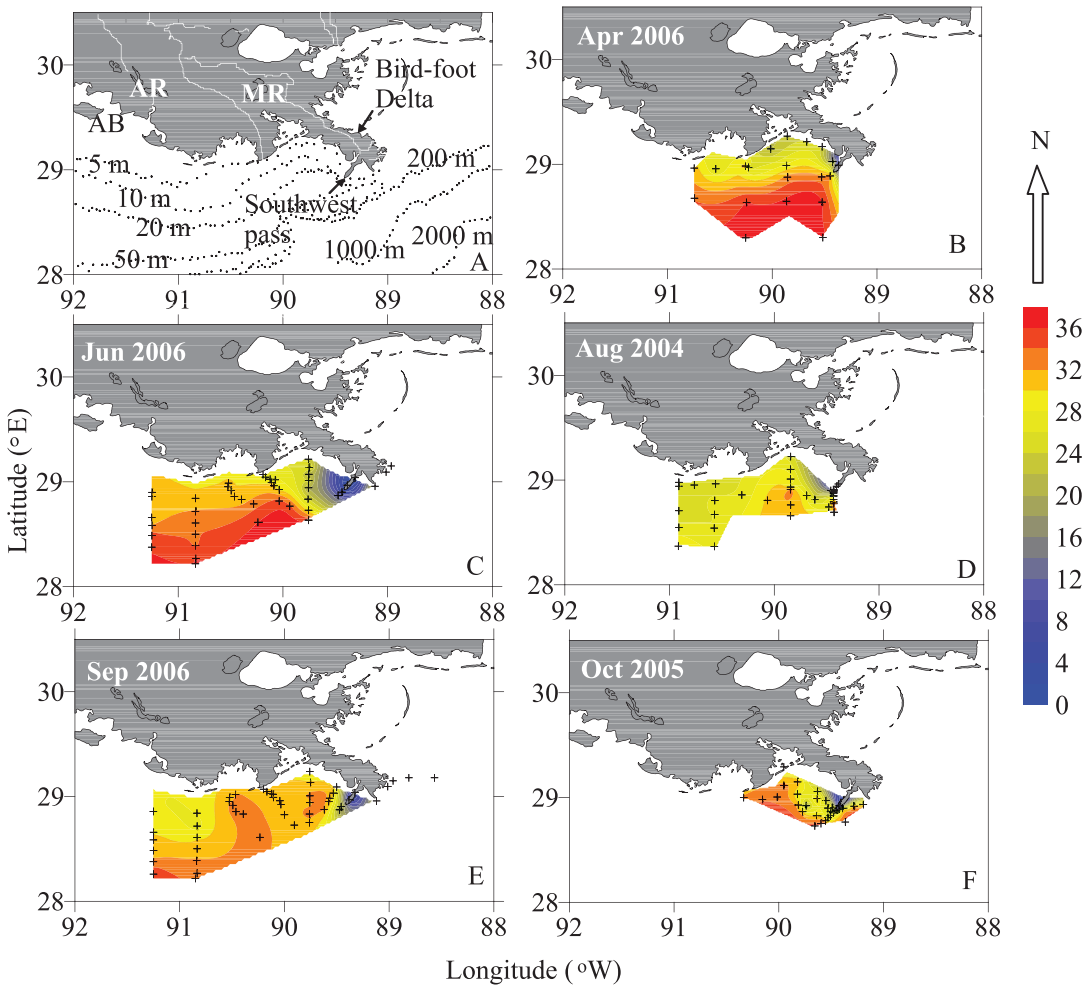

Fig. 1. Map of (A) the Mississippi River plume and contours of isohalines marked with sampling stations (crosses) for the cruises of (B) April 2006, (C) June 2006, (D) August 2004, (E) September 2006, and (F) October 2005. In (A), MR and AR represent the Mississippi River and Atchafalaya River, respectively; AB denotes Atchafalaya Bay.

samples were collected into 60-mL glass bottles with polyvinyl-lined closures. Samples for DIC were collected into 120-mL glass bottles and poisoned with 50 μL of saturated $HgCl_2$ solution.

Analytical methods and data processing—DIC was measured by acidification and subsequent quantification of released CO_2 with a CO_2 detector (Li-Cor® 6262) to a precision of $\pm$ 2 μmol kg^{-1}. DIC measurements were calibrated against certified reference materials provided by A. G. Dickson of Scripps Institution of Oceanography.

Samples for pH were placed into a 25 $\pm$ 0.05°C bath for about 30 min and subsequently measured with an Accumet® 20 or 25 pH meter fitted with an Orion Ross® combination pH electrode (8102BN). The pH system was calibrated against three National Institute of Standards and Technology–traceable pH buffers (4.00, 7.00, and 10.00 at 25°C from Fisher Scientific). The precision of the pH measurement was $\pm$ 0.005. All the pH analyses were conducted onboard ship within 1 h of sampling.

TAlk was calculated from DIC and pH with the program developed for CO_2 system calculations (CO2SYS; Lewis and Wallace 1998). The dissociation constants of carbonic acid were taken from Millero et al. (2006) for estuarine waters. The CO_2 solubility coefficient was taken from Weiss (1974) and the sulfate dissociation constant from Dickson (1990).

For the April 2006 and October 2005 cruises, DO samples were determined by the Winkler spectrophotometric method (Pai et al. 1993), with an accuracy of $\pm$ 2 μmol O_2 kg^{-1}. For the June and September 2006 cruises, DO was measured with an Orion® 862A DO meter calibrated against water-saturated air. DO concentrations were also measured using Winkler titration on a subset of samples. The results from the DO meter were calibrated against the Winkler DO data ($DO_{Winkler} = 1.02 \times DO_{Benchtop} + 0.48$, $R^2 = 0.96$, $n = 27$ for June 2006 cruise, and $DO_{Winkler} = 1.02 \times DO_{Benchtop} + 0.19$, $R^2 = 0.99$, $n = 34$ for September 2006 cruise). For the August 2004 cruise, DO was measured with a Wissenschaftlich-Technische-Werkstätten (WTW®)

Multi Meter and CellOx 325 DO probe calibrated against water-saturated air.

The calcite or aragonite saturation index (Ω) was calculated from Ca^{2+} and CO_3^{2-} concentrations in the water, i.e., $\Omega = [Ca^{2+}][CO_3^{2-}]/K_{sp}$, where K_{sp} is the $CaCO_3$ solubility product from Mucci (1983). Ca^{2+} concentrations were calculated assuming multiple end-member mixing between Mississippi and Atchafalaya River waters and seawater similar to the TAlk mixing (*see* below). The concentrations of Ca^{2+} in the Mississippi and Atchafalaya Rivers were from U.S. Geological Survey (USGS) monitoring data (890–1144 μmol kg^{-1} in the Mississippi River, USGS Sta. 07373420, and 823–1120 μmol kg^{-1} in the Atchafalaya River, USGS Sta. 07381495). Ca^{2+} in seawater was derived from the observed salinity (S) at the seawater end member during the cruises assuming a constant Ca : S ratio (Millero 2005). CO_3^{2-} concentration was calculated from DIC and pH with the program CO2SYS (Lewis and Wallace 1998) using the same constants as with the TAlk calculation.

Mixing, mass balance, and NCP calculation

Three–end-member mixing model—As TAlk values in the Mississippi River and the Atchafalaya River may be different (*see River end-member values and fluxes* in the Results section), we use a three–end-member mixing model to interpret the DIC and TAlk distributions. First, we have

$$f_{R1} + f_{R2} + f_{sw} = 1 \quad (1)$$

where f_{R1}, f_{R2}, and f_{sw} represent the fraction corresponding to the Mississippi River, the Atchafalaya River, and seawater, respectively. The salinity and TAlk budgets can then be expressed as

$$S = S_{R1} \times f_{R1} + S_{R2} \times f_{R2} + S_{sw} \times f_{sw} \quad (2)$$

and

$$TAlk = TAlk_{R1} \times f_{R1} + TAlk_{R2} \times f_{R2} + TAlk_{sw} \times f_{sw} \quad (3)$$

where S and TAlk of the different end members are designated by the subscripts R1 for the Mississippi River, R2 for the Atchafalaya River, and sw for seawater.

For the DIC budget, in addition to mixing, there are changes due to net OC production and consumption (ΔDIC_{OC}) and gas exchange ($\Delta DIC_{air-sea}$). The DIC budget can thus be expressed as

$$DIC = DIC_{R1} \times f_{R1} + DIC_{R2} \times f_{R2} + DIC_{sw} \times f_{sw} + \Delta DIC_{OC} + \Delta DIC_{air-sea} \quad (4)$$

Subtracting Eq. 4 from Eq. 3 and rearranging:

$$\Delta DIC_{OC} = f_{R1} \times (TAlk_{R1} - DIC_{R1}) + f_{R2} \times (TAlk_{R2} - DIC_{R2}) + f_{sw} \times (TAlk_{sw} - DIC_{sw}) - (TAlk - DIC) - \Delta DIC_{air-sea} \quad (5)$$

where $\Delta DIC_{air-sea}$ can be calculated from ΔpCO_2, the difference in pCO_2 between the water and the atmosphere, and wind speed (hourly-averaged data provided by ship's log) using a thin-layer diffusion model (Wanninkhof 1992) combining the mixed-layer depth and water residence time. From the above equation, it is clear that we use TAlk to take care of the multiple–end-member mixing issue and attribute the relative difference between DIC and TAlk to nonconservative DIC changes.

As will be discussed later (Eq. 10 in the Discussion), biological production and respiration of OC also has a small contribution to alkalinity; we thus amend Eq. 3 by adding the term $-17/106 \times \Delta DIC_{oc}$. Equations 1–5 can then be solved simultaneously.

Estimating NCP based on a box-model approach—Values of ΔDIC_{OC} presented above reflect the accumulated biological uptake of DIC during plume transit, but not the net rate in a specific subregion of interest. To estimate NCP in a plume subregion, we used the DIC mass balances in a box-model formulation. In order to estimate NCP with some spatial resolution, we divided the plume into four subregions as in Green et al. (2006). The physical characteristics of these are presented in the Results section. We assumed each box or subregion gains water and dissolved constituents (i.e., salt and DIC) only from its upstream box and the ocean water (Ledwell et al. 1993; Fig. 2). For each box, we first used a salt budget to calculate the ratio of water from the upstream box and from the ocean end member. Then, based on DIC mass balance, we calculated the amount of nonconservative DIC changes in each box (ΔDIC_i), which were due to biological uptake and air–sea exchange. Next, the DIC change due to OC production in each box ($\Delta DIC_{OC,i}$) was obtained by subtracting a small amount of DIC change resulted from air–sea CO_2 exchange ($\Delta DIC_{air-sea,i}$). Finally, NCP in each box (NCP_i) was estimated from the $\Delta DIC_{OC,i}$, the plume mixed-layer depth (MLD_i), and the water residence time (τ_i), i.e., $NCP_i = \Delta DIC_{OC,i} \times MLD_i/\tau_i$. Here, with a NCP unit of g C m^{-2} d^{-1}, the area dimension is cancelled out.

Specifically, for the salt balance of box A in Fig. 2, we have

$$S_{R1} \times Q_{R1} + S_{R2} \times Q_{R2} + S_{sw} \times Q_{sw,A} = S_A \times (Q_{R1} + Q_{R2} + Q_{sw,A}) \quad (6)$$

in which, S_{R1}, S_{R2}, S_{sw}, S_A, Q_{R1}, Q_{R2}, and $Q_{sw,A}$ are salinity of river 1 (Mississippi), salinity of river 2 (Atchafalaya), salinity of seawater, average salinity of box A, freshwater flux of river 1, freshwater flux of river 2, and flux of seawater into box A. The ratio of freshwater from the two rivers was determined from the three–end-member mixing model described earlier.

At steady state, the total water flux into box A, Q_A, equals the sum of river inputs and seawater input (Q_{R1} + Q_{R2} + $Q_{sw,A}$). As both S_{R1} and S_{R2} are 0, from Eq. 6, we have

$$Q_{sw,A} = S_1 \times (Q_{R1} + Q_{R2})/(S_{sw} - S_A) \quad (7)$$

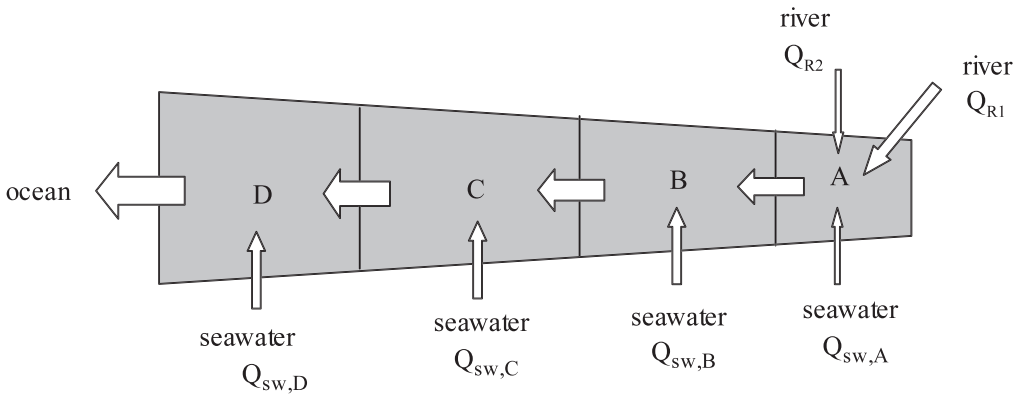

Fig. 2. Illustration of the box model for the NCP estimation of the Mississippi River plume. Boxes A, B, C, and D represent the salinity ranges 0–18, 18–27, 27–32, and 32–34.5, respectively. They represent subregions 1, 2, 3, and 4 in the text. The widths of the arrows are not exactly proportional to the actual values.

For DIC balance, we have

$$\begin{aligned} &DIC_{R1} \times Q_{R1} + DIC_{R2} \times Q_{R2} + DIC_{sw} \\ &\quad \times Q_{sw,A} + \Delta DIC_A \times (Q_{R1} + Q_{R2} + Q_{sw,A}) \\ &\quad = DIC_A \times (Q_{R1} + Q_{R2} + Q_{sw,A}) \end{aligned} \quad (8)$$

Here ΔDIC_A is the overall DIC change in box A, which includes OC production and respiration ($\Delta DIC_{OC,A}$) and gas exchange ($\Delta DIC_{air-sea,A}$). Rearranging Eq. 8 yields

$$\begin{aligned} \Delta DIC_A = DIC_A - (&DIC_{R1} \times Q_{R1} + DIC_{R2} \times Q_{R2} \\ &+ DIC_{sw} \times Q_{sw,A})/(Q_{R1} + Q_{R2} + Q_{sw,A}) \end{aligned} \quad (9)$$

The $\Delta DIC_{oc,A}$ term can subsequently be derived by subtracting the relatively small gas exchange term, $\Delta DIC_{air-sea,A}$. Similarly, we can derive ΔDIC_i and $\Delta DIC_{OC,i}$ for boxes B, C, and D, with replacing river outflow by the outflow of the upstream box.

Results

River end-member values and fluxes—The freshwater discharge from the Mississippi River exhibited typical seasonality with peak flow in late winter and spring, decreasing flow through midsummer, and lowest flow in late summer and fall (Fig. 3A). However, TAlk in the river varied in a pattern opposite to that of freshwater discharge (Fig. 3B). Mississippi River DIN concentrations and loads also show significant seasonal variations, with highest values occurring in late spring and early summer and lagging 1–2 months behind the peak of freshwater discharge (Fig. 3B,C).

Discharge from the Atchafalaya River had a similar seasonal pattern to that of the Mississippi River, but TAlk in the Atchafalaya River was lower than that of the Mississippi River in most cases. For example, during flood season TAlk in the Atchafalaya River was 300–700 μmol kg^{-1} lower than that in the Mississippi River (Fig. 3B). The lower TAlk in the Atchafalaya River was attributed to dilution by Red River water, which has a characteristically lower TAlk (1100–2500 μmol kg^{-1}, USGS Sta. 07355500).

The USGS TAlk values in the Mississippi and Atchafalaya Rivers for the sampling periods are presented in Table 1. As DIC values are not available from the USGS, we assumed that river end-member DIC was 30 μmol kg^{-1} higher than TAlk in all seasons for both rivers. This assumption is consistent with our observations of the relationship between TAlk and DIC in the low-salinity plume (*see* section that follows, "*Spatial distributions of DIC, TAlk, pH, DO, and $CaCO_3$ saturation index*"). With these TAlk and DIC values, the calculated river end-member pCO_2 was 100–150 Pa, which is similar to the observed pCO_2 range in the lower Mississippi River (Dagg et al. 2005; W.-J. Cai unpubl.). As DIC values were not available for most rivers, this is a useful and reasonable assumption for other rivers as well (i.e., Eq. 5 will be applicable to estuarine and plume mixing cases with unknown river end-member values).

Plume hydrographic properties—Salinity in the plume was generally low near the river outflow region. Surface salinity at the mouth of the Mississippi River ranged from < 1 to 6 depending on the level of river discharge. In April and June 2006, surface salinity isohalines were oriented parallel with the coast (Fig. 1B,C); a large region of low-salinity water was evident near the river mouth in June 2006. In October 2005, the surveyed area was limited to the Louisiana Bight region, when the plume was evidently westward of the delta and salinities were higher than in April or June 2006 (Fig. 1F), a result consistent with the relatively low freshwater discharge during that time. In August 2004, the plume extended farther offshore than in April or June 2006 (Fig. 1D). In September 2006, an additional region of low-salinity water was evident at the western edge of the survey area, likely because of the Atchafalaya River outflow (Fig. 1E).

Surface water temperatures varied in a typical seasonal fashion, ranging from 21.2°C to 26.1°C in April 2006,

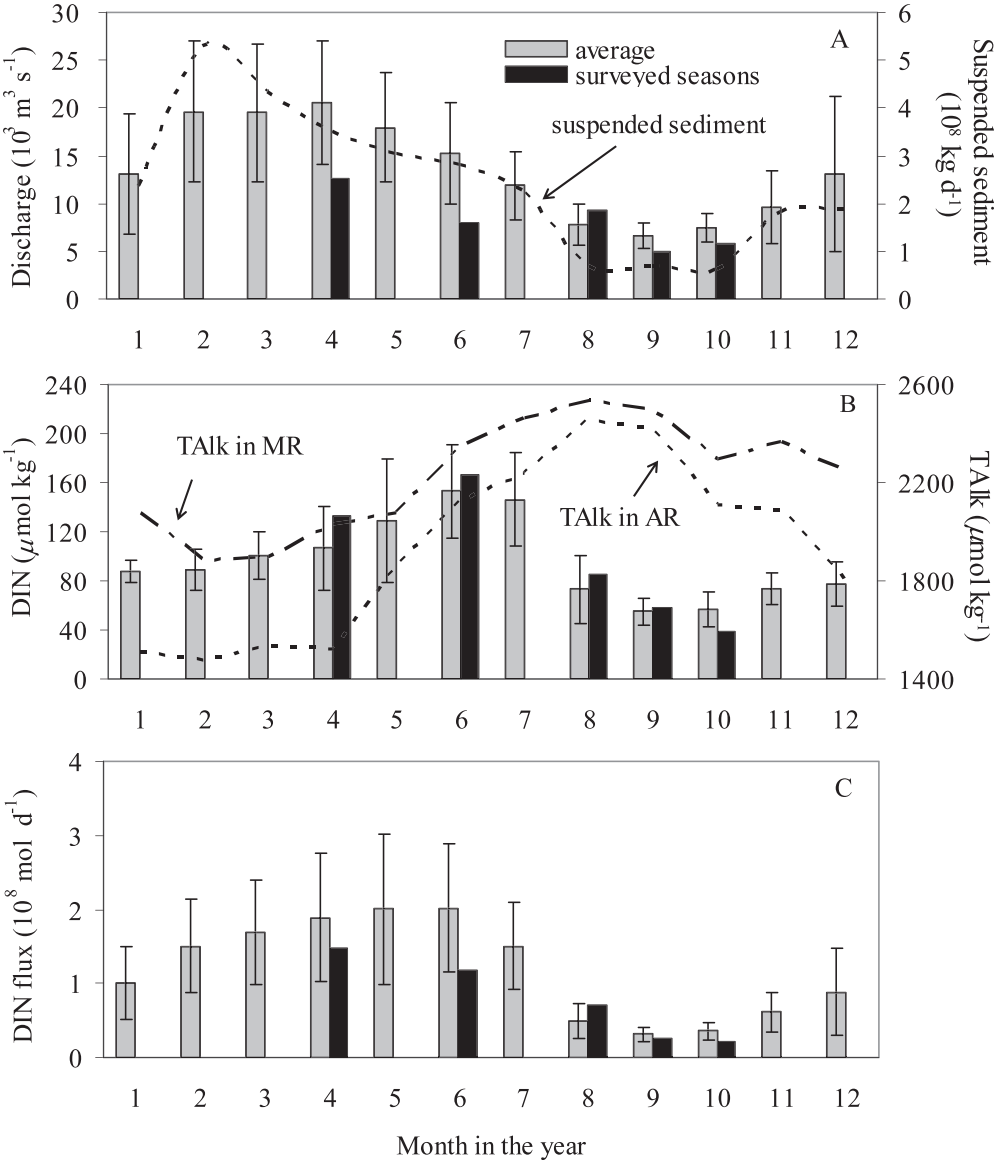

Fig. 3. (A) Freshwater discharge of long-term monthly average (grey bars) and for months of cruises (black bars) and suspended sediment load (dashed line), (B) Average monthly DIN (NO_3^- + NO_2^- + NH_4^+) (grey bars) and for months of cruises (black bars), and TAlk concentrations for the Mississippi (MR, long dashed line) and Atchafalaya (AR, short dashed line) Rivers, and (C) Average monthly DIN fluxes (gray bars) and for months of cruises (black bars). All averages were for the period of 1997–2006 with error bars representing the standard deviation. Data were primarily from the Mississippi River at St. Francisville (USGS Sta. 07373420, near St. Francisville, Louisiana, at 30°45′30″ N, 91°23′45″ W) except for the Atchafalaya River TAlk. The Atchafalaya River TAlk data were from the Atchafalaya River at Melville (USGS Sta. 07381495 at 30°41′26″ N, 91°44′10″ W). All data were from USGS web page, "Water-Quality Data for the Nation" (http://waterdata.usgs.gov/nwis/qw).

25.6°C to 30.0°C in June 2006, 29.0°C to 31.5°C in August 2004, 29.5°C to 31.7°C in September 2006, and 26.4°C to 28.7°C in October 2005.

Physical characteristics of plume subregions—Total plume area was calculated from the relationship with river discharge as developed by Green et al. (2006). This was further partitioned into the four regions according to Green et al. (2006) (Table 2). The four plume subregions were defined by salinity ranges of 0–18, 18–27, 27–32, and 32–34.5, respectively (Green et al. 2006). Freshwater residence times of each subregion were adopted from Green et al. (2006) (Table 2). Mixed-layer depths were calculated as the depth at which the potential density change exceeded 0.125 m^{-1} (Levitus 1982) (Table 2). The plume area, so estimated, ranged from 1080 to 1820 km^2, and the mixed-

Table 1. End-member values of salinity, DIC, and TAlk in the rivers and seawater.

	End-member 1 (Mississippi River)*			End-member 2 (Atchafalaya River)†			End-member 3 (ocean)		
Survey	TAlk (μmol kg^{-1})	DIC (μmol kg^{-1})	Discharge (m^3 s^{-1})	TAlk (μmol kg^{-1})	DIC (μmol kg^{-1})	Discharge (m^3 s^{-1})	Salinity	TAlk (μmol kg^{-1})	DIC (μmol kg^{-1})
Apr 2006	2330	2360	12,600	1750	1780	5400	36.5	2398	2052
Jun 2006	2700	2730	8000	2500	2530	3300	36.1	2410	2070
Aug 2004	2500	2530	9200	2200	2230	4000	33.6	2347	2000
Sep 2006	2430	2460	5000	2430	2460	2000	35.7	2397	2029
Oct 2005	2400‡	2430	5800	2100	2130	2000	34.9	2313	1991

* Mississippi River at St. Francisville (USGS Sta. 07373420), Louisiana. Data are from the USGS Web page "Water-Quality Data for the Nation" (http://waterdata.usgs.gov/nwis/qw).
† Atchafalaya River at Melville (USGS Sta. 07381495), Louisiana. Data are from the USGS Web page "Water-Quality Data for the Nation" (http://waterdata.usgs.gov/nwis/qw).
‡ The USGS value was not used here; rather, the value was extrapolated from the TAlk distribution pattern in the plume.

layer depth ranged from 2 to 8 m. These estimates were similar to the historical averages given in earlier work (Green et al. 2006). Thus, we believe that our plume conditions were similar to the historical average and it was therefore reasonable to use the average water residence times given in Green et al. (2006).

Spatial distributions of DIC, TAlk, pH, DO, and $CaCO_3$ saturation index—During the surveys, the Mississippi River water had DIC and TAlk values higher than or similar to the surface seawater of the northern Gulf of Mexico (Fig. 4). In the low-salinity area, DIC was 2400–2600 μmol kg^{-1}, decreasing with increasing salinity to a minimum of $\sim$ 1850 μmol kg^{-1} at mid salinities, and then increasing to 1990–2075 μmol kg^{-1} at the seawater end member. TAlk at the mouth of the Mississippi River was 30–50 μmol kg^{-1} lower than DIC and tended to decrease slightly at mid-salinity before increasing to the seawater value. A mid-salinity minimum in TAlk was observed in June 2006, August 2004, and October 2005.

Table 2. Physical background information of the Mississippi River plume.

Season	Survey	River discharge (m^3 s^{-1})*	Plume area (10^3 km^2)†	Subregion	Salinity	Subregion area (%)‡	Subregion area (10^3 km^2)	Water residence time (d)‡	Mixed-layer depth (m)
Spring	Apr 2006	12,600	1.82	1	0–18	35	0.64	1	3
				2	18–27	25	0.45	1.5	4
				3	27–32	20	0.36	6	6
				4	32–34.5	20	0.36	6	5
				Sum	—	100	1.82	—	—
Summer	Jun 2006	8000	1.37	1	0–18	15	0.21	1	2
				2	18–27	45	0.62	1.5	3
				3	27–32	20	0.27	6	3
				4	32–34.5	20	0.27	6	2
				Sum	—	100	1.37	—	—
	Aug 2004	9200	1.49	1	0–18	15	0.22	1	3
				2	18–27	45	0.67	1.5	4
				3	27–32	20	0.30	6	4
				4	32–34.5	20	0.30	6	3
				Sum	—	100	1.49	—	—
Fall	Sep 2006	5000	1.08	1	0–18	15	0.16	1	3
				2	18–27	35	0.38	1.5	3
				3	27–32	25	0.27	6	5
				4	32–34.5	25	0.27	6	8
				Sum	—	100	1.08	—	—
	Oct 2005	5800	1.16	1	0–18	15	0.17	1	4
				2	18–27	35	0.41	1.5	5
				3	27–32	25	0.29	6	7
				4	32–34.5	25	0.29	6	8
				Sum	—	100	1.16	—	—

* Freshwater discharge from Mississippi River at St. Francisville (USGS Sta. 07373420), Louisiana. Data are from the USGS Web page "Water-Quality Data for the Nation" (http://waterdata.usgs.gov/nwis/qw).
† Calculated using formula of plume area as a function of river discharge, plume area (m^2) = $9.67 \times 10^4 \times$ river discharge (m^3 s^{-1}) + 5.94×10^8, $r^2 = 0.63$ (Green et al. 2006).
‡ From Green et al. (2006).

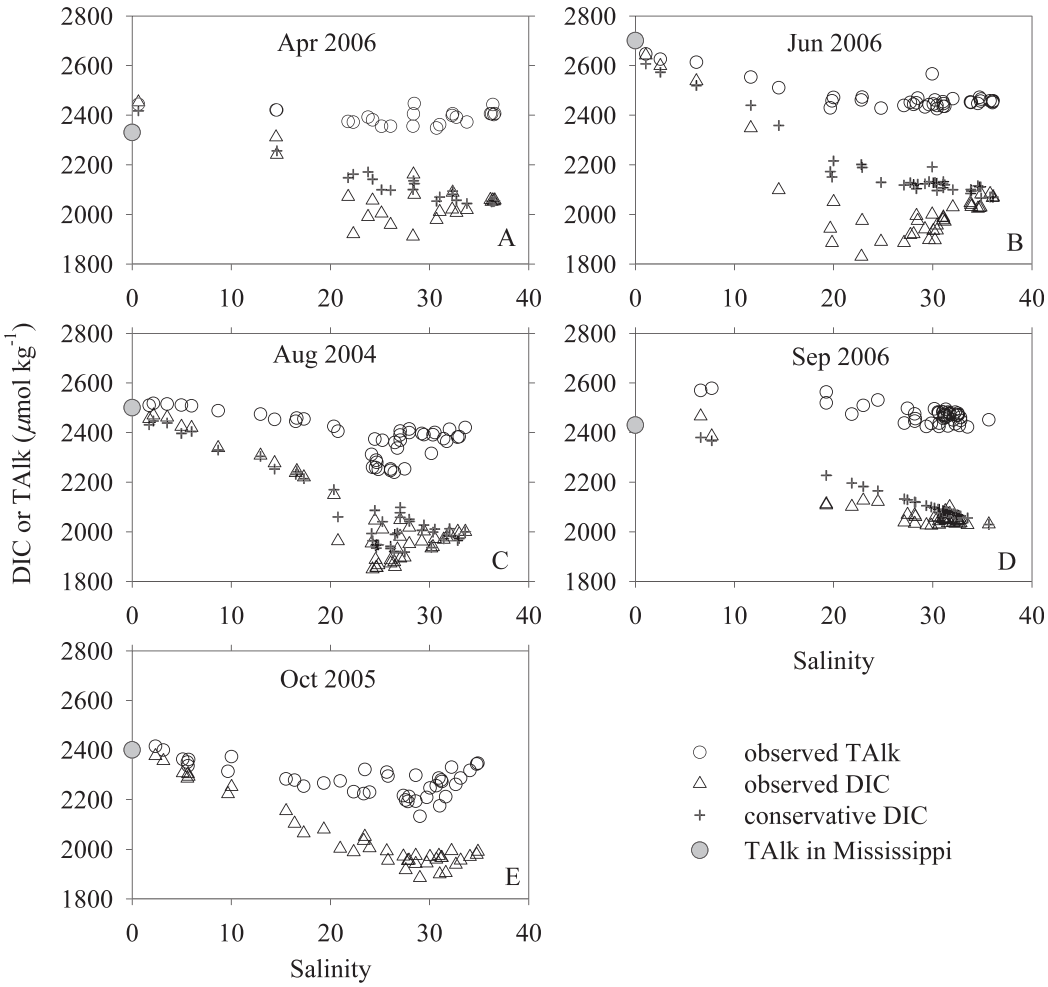

Fig. 4. Distributions of DIC and TAlk of surface water along salinity gradient in the Mississippi River plume. The gray solid circles at salinity 0 represent the USGS TAlk values of the Mississippi River (USGS Sta. 07373420) except for October 2005. The crosses represent the conservative DIC according to the three–end-member mixing model. The USGS data were from the USGS web page, "Water-Quality Data for the Nation" (http://waterdata.usgs.gov/nwis/qw).

In general, USGS Mississippi River TAlk values were consistent with extrapolations from our observed TAlk–salinity mixing lines in mid- to low-salinity area (Fig. 4), except for October 2005, when USGS datum of 2200 μmol kg^{-1} was much lower than the 2400 μmol kg^{-1} expected from the mixing line. We assumed 2400 μmol kg^{-1} as the Mississippi River end member to calculate the $CaCO_3$ saturation index, but excluded this cruise from the NCP calculation as it might reflect atypical conditions following two major hurricanes.

Distributions of surface-water pH contrasted with those of DIC, being lowest at low salinities ($\sim$ 7.91), peaking at mid salinities (8.10–8.74), and decreasing in offshore waters (8.20–8.26; Fig. 5). The highest pH was observed in June 2006 and August 2004. Distributions of DO saturation were similar to those of pH, being lowest at low salinities (82–99%) and higher at mid salinities (75–180%) and decreasing at high salinities (102–108%; Fig. 5).

The salinity relationships of aragonite and calcite saturation indices were similar to those of pH (Fig. 6). For aragonite, the saturation index was $\sim$ 1 at low salinity, increased to 3–8 at mid salinities, and decreased to $\sim$ 4 at the seawater end member. For calcite, the saturation index was always higher (by 1.5 times), but otherwise showed the same pattern as aragonite. The highest saturation index was observed in April 2006, June 2006, and August 2004 (Fig. 6).

Discussion

Conservative mixing scheme in the plume—A major consideration in our analyses was what end-member terms were involved in mixing between river and ocean water, as this was required for calculating biological CO_2 removal rates in the plume. Various past studies have assumed a two–end-member mixing model in the Mississippi River plume to examine biological nutrient removal (Hitchcock et al. 1997). Lohrenz et al. (1999) observed that nonconservative behavior in nutrient–salinity relationships coincided with peaks in primary productivity. In contrast, relationships between DOC and salinity tend to be more conservative (Del Castillo and Miller 2008). Cai (2003)

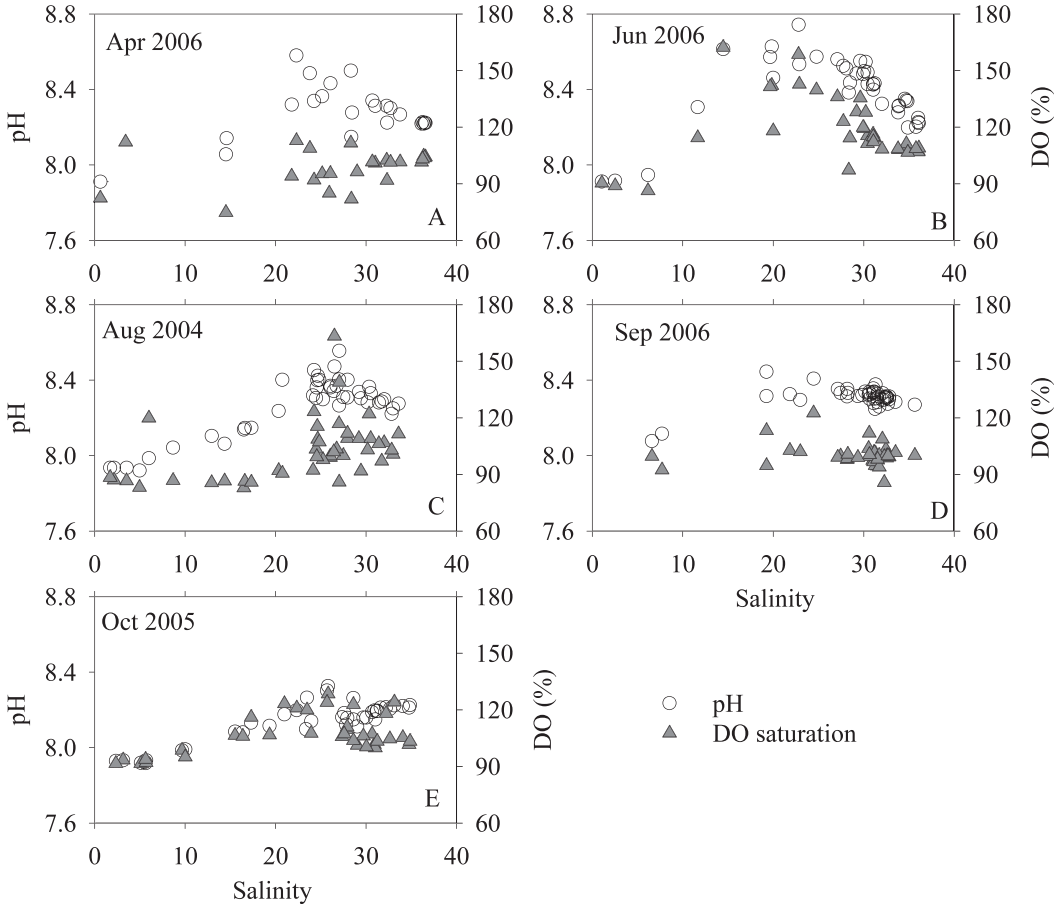

Fig. 5. Distributions of pH and DO saturation (%) along salinity gradient in the Mississippi River plume during the five surveyed seasons.

used a two–end-member mixing model to estimate biological uptake in the Mississippi River plume, although that study was more geographically restricted to the region near the Southwest Pass. Based on observations in August and September 1998, Cai and Lohrenz (2010) concluded that the water chemistry of the Atchafalaya River was similar to that of the Mississippi River and thus the two rivers could be combined into one freshwater end member.

If the Mississippi River plume was indeed behaving as a two–end-member mixing system in all seasons, the observed TAlk deficit in mid-salinity areas could be interpreted as due to in situ calcification. Two pieces of evidence had led us to postulate this interpretation. First, previous studies demonstrated that prymnesiophytes can be abundant in this area (Wysocki et al. 2006), and some types of prymnesiophytes, specifically coccolithophores, precipitate $CaCO_3$. Second, we observed coccoliths in filtered particle samples at some stations collected during June 2006 (W.-J. Cai unpubl.). We evaluated this possibility by analyzing the Ca^{2+} : Na^{+} ratios in the filters from several stations across the salinity gradient. However, the Ca^{2+} : Na^{+} ratios of the acid extract of filtered particles indicate that calcification was not sufficient in magnitude to alter the TAlk–salinity relationship (W.-J. Cai unpubl.).

The earlier conclusion of similar TAlk values in the two rivers (Cai and Lohrenz 2010) was based on surveys of limited times (August and September of 1998 during a low discharge period) and areas. However, our more extensive observations make it clear that Atchafalaya River TAlk values are consistently lower than those of the Mississippi River, especially during periods of high river discharge (Fig. 3B). By considering both Mississippi and Atchafalaya River end-member TAlk values within the period of 2 weeks prior to the survey, we found that the observed TAlk values were all within the triangle of the three end members for all cruises except for October 2005. Therefore, we concluded that the nonlinear TAlk and salinity relationship could be explained by a three–end-member mixing process, and secondarily may be attributable to temporal variation in TAlk concentrations of the river end members. We therefore further concluded that calcification was not a major process affecting the TAlk distribution.

For October 2005, there were two additional factors that may have affected the results. Hurricanes Katrina and Rita introduced substantial amounts of coastal wetland runoff to the area, thus potentially serving as another end member. Disturbance of the bottom water and sediments due to hurricane-induced currents and waves occurred and may have been accompanied by an oxidation of reduced sulfur products that could also reduce TAlk. As we cannot verify the exact cause, we will not discuss this further.

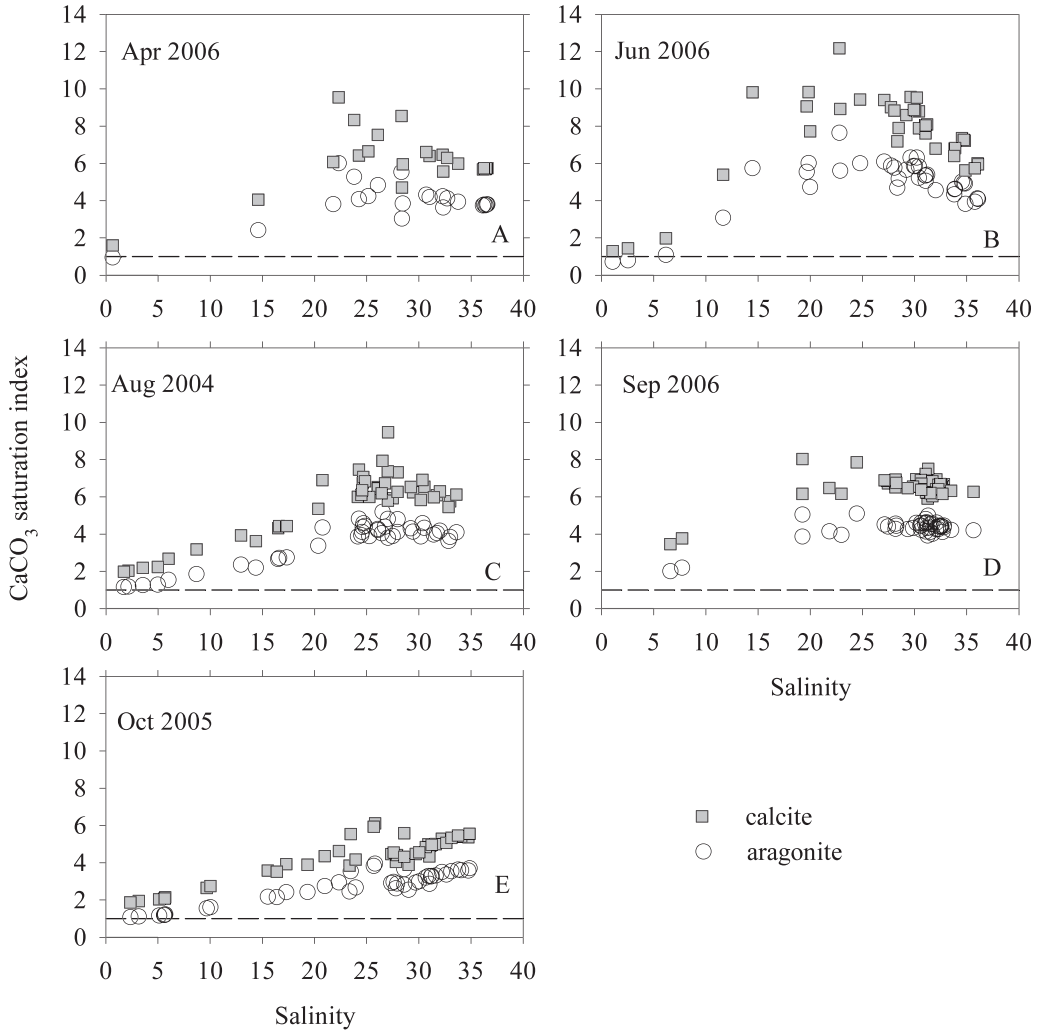

Fig. 6. Distributions of the saturation index (Ω) of $CaCO_3$ in the Mississippi River plume in the surveyed seasons. The horizontal dashed lines represent the 100% saturation ($\Omega = 1$), where $\Omega = ([Ca^{2+}] \times [CO_3^{2-}])/K_{sp}$, and in which K_{sp} is the stoichiometric solubility product for a particular mineral phase of $CaCO_3$.

Finally, it should also be noted that Lohrenz et al. (1999) argued that the exchange of plume surface water with subsurface water of intermediate salinity may complicate the mixing scenario. Although the mid-water layer is ultimately the result of mixing of the end members, it is representative of processes that occurred over a longer time scale than that of surface plume water. Thus, this could introduce uncertainty in quantifying rates of biological activities, particularly if the river end member undergoes a significant change in properties over this longer time scale. This issue deserves further study.

Processes influencing pH, DIC, and TAlk distributions—Comparisons of the observed DIC and calculated conservative DIC from the three–end-member mixing model provided evidence of biological removal (Fig. 4). At intermediate salinities, observed DIC was lower than the conservative DIC, especially for the April 2006 and June 2006 cruises. According to the idealized Redfield stoichiometry, biological production or respiration of organic matter can be represented as

$$(CH_2O)_{106}(NH_3)_{16}(H_3PO_4) + 138O_2 \leftrightarrow 106CO_2 + 16NO_3^- + H_2PO_4^- + 17H^+ + 122H_2O \quad (10)$$

This process controls nonconservative DIC change but affects TAlk only slightly, in a ratio of approximately $-17:106$ of TAlk to DIC mainly because of the change of the oxidation state of N (i.e., Organic N $\rightarrow$ $NH_3 + 2O_2 \rightarrow NO_3^- + H^+ + H_2O$). Prior studies have argued that TAlk combined with NO_3^- concentration, the so-called potential TAlk (TAlk + NO_3^-), can be used as a conservative tracer for biological release of DIC (Brewer et al. 1975). We must point out that over a salinity gradient in an estuary or a plume, the NO_3^- concentration change is a result of both mixing and biological removal. Only the latter contributes to the alkalinity balance. We thus amended Eq. 3 by adding a term, $-17/106 \times \Delta DIC_{oc}$, where ΔDIC_{oc} is the simultaneous biological removal of DIC and NO_3 accord-

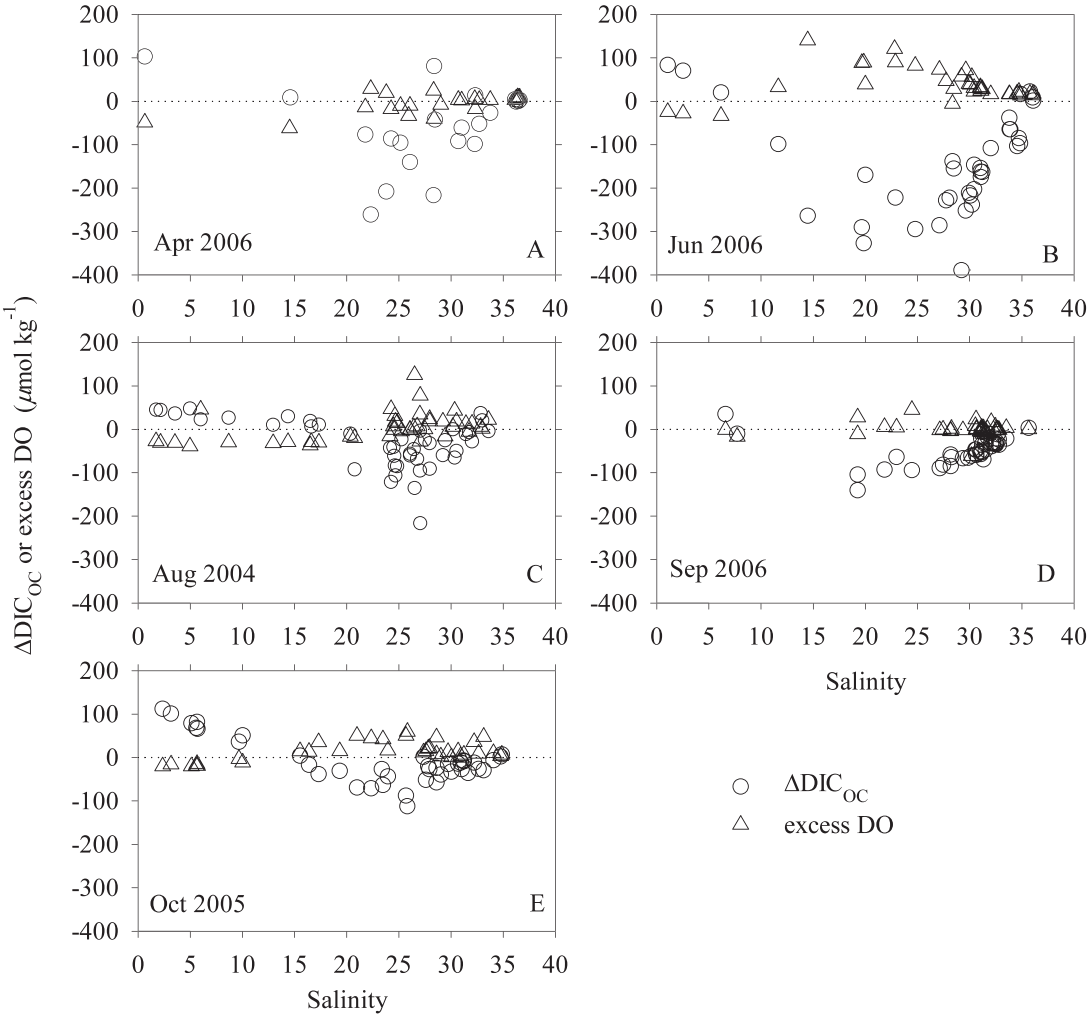

Fig. 7. A comparison of excess DO and ΔDIC_{OC} in the Mississippi River plume, where excess DO was the difference between the observed DO and the calculated saturated DO. The DO saturation was calculated based on the empirical formula of Benson and Krause (1984).

ing to the Redfield ratio, which would result in a small TAlk increase. The equations were then solved simultaneously. For the maximum ΔDIC_{oc} cruise (-310 μmol kg^{-1} in June 2006), the maximum contribution of biological production to TAlk is about + 50 μmol kg^{-1}, a small but nontrivial contribution.

The DIC removal and nutrient depletion (data not presented) observed at intermediate salinities were consistent with the expected high primary productivity for this region (Lohrenz et al. 1999; Lehrter et al. 2009). Earlier studies have suggested that much of the community respiration in the plume is supported by primary production within the plume rather than by riverine inputs of terrestrial organic matter (Gardner et al. 1994). Therefore, photosynthesis and respiration are the major processes influencing carbonate system properties, and they are closely coupled in the Mississippi River plume (Gardner et al. 1994).

Similar to DIC and TAlk distributions, high DO and high pH values in the mid-salinity zone reflect the biological processes in the plume. As predicted by Eq. 10, DO increase should be similar to DIC decrease and pH should increase as a result of biological CO_2 fixation. Although, in general, excess DO (the difference between observed DO and calculated DO saturation) mirrored ΔDIC_{OC}, excess DO was lower than that expected from ΔDIC_{OC} (Fig. 7). This could be explained by the shorter time scale required for oxygen equilibration with the atmosphere (about 1 week) than for CO_2 and DIC (a few months).

Another process that can alter TAlk distributions is the oxidation of NH_4^+ to NO_3^-. Note that the oxidation of ammonia released from organic matter was already accounted for in Eq. 10 and thus should not be counted again in the TAlk budget. However, oxidation of NH_4^+ originating from rivers will affect TAlk. As NH_4^+ concentrations in the lower Mississippi River are typically low (< 3 μmol kg^{-1}, USGS Sta. 07373420), we ignored this effect. Similarly, other processes such as denitrification and sulfate reduction can potentially influence TAlk distributions, but these are unlikely to occur in oxygenated surface plume waters. In summary, we conclude that photosynthe-

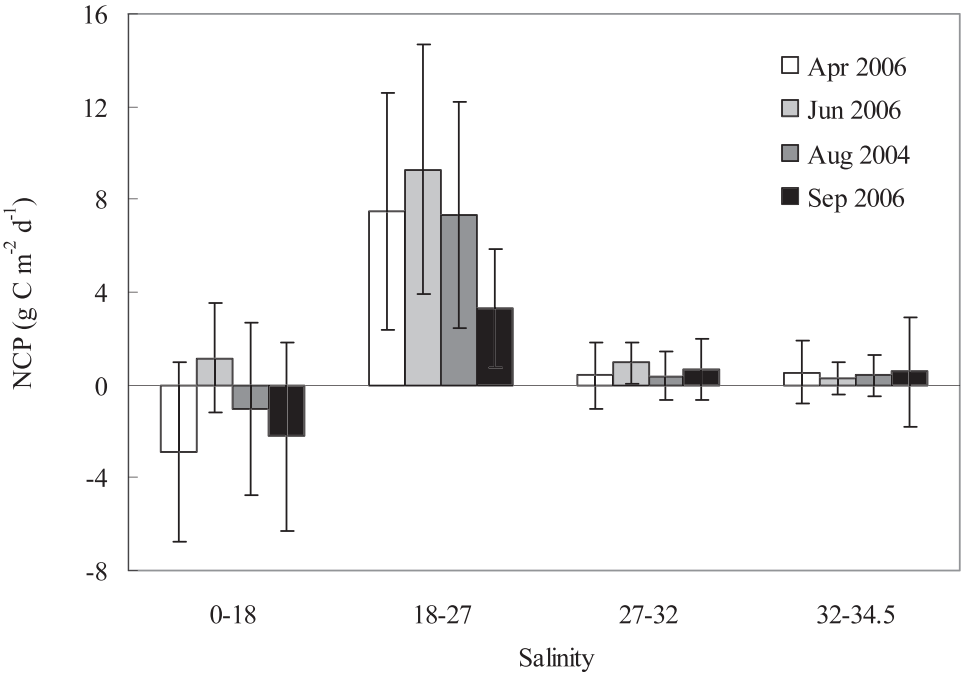

Fig. 8. Calculated NCP rates in the four subregions of the Mississippi River plume in the surveyed seasons. The error bars represent the standard deviation.

sis and aerobic respiration were the dominant biological processes influencing spatial and temporal distributions of DIC in the upper mixed layer of the Mississippi River plume and surrounding areas.

Carbonate saturation state—The carbonate saturation state of coastal ocean waters has become an important topic because of the scientific interest and societal concerns about the effects of ocean acidification (Kleypas et al. 1999; Feely et al. 2008; Salisbury et al. 2008). The carbonate saturation index provides a useful parameter for describing the conditions of the carbonate system in water. Based on thermodynamic prediction of water mixing alone, Salisbury et al. (2008) argued that river plumes, including that of the Mississippi River, can be a factor causing low pH and low saturation state, and can affect the health of aragonite shell-bearing organisms in coastal oceans. We did observe relatively low values of aragonite saturation in the low-salinity region near the river mouth (Fig. 6). However, in contrast to Salisbury et al. (2008), our results support the view that large river plumes can have high carbonate saturation states in the upper mixed layer. For example, at intermediate salinities of the Mississippi River plume where pH was high, the saturation index was 5–12 for calcite and 3–7 for aragonite during our cruises (Fig. 6), which is significantly higher than the average saturation state of subtropical surface seawater (5–6 for calcite and 3–4 for aragonite in subtropical surface seawater; Kleypas et al. 1999). A recent modeling study in Belgian coastal waters (Borges and Gypens 2010) and observations from the Changjiang plume (Chou et al. 2009*a*; Zhai and Dai 2009) are consistent with our observations in the Mississippi River plume.

The $CaCO_3$ saturation state in the low-salinity plume region of the Mississippi River was high compared to the plumes of the Kennebec, Congo, Amazon, and other rivers (Salisbury et al. 2008), which was mainly attributable to the high carbonate content of the Mississippi River waters. However, in mid- to high-salinity areas, biological control of pH (Fig. 5) played a dominant role in carbonate saturation states. This was not considered in the mixing model of Salisbury et al. (2008). The distribution of $CaCO_3$ saturation state was similar to that of O_2, pH (Figs. 5, 6), and chlorophyll *a* (Lehrter et al. 2009), that is, exhibiting a mid-salinity maximum. Further evidence of biological control was the fact that seasonal patterns of saturation state of both calcite and aragonite were similar to that of NCP (*see* following section, *NCP and its spatiotemporal variation*) being higher in summer than in spring and fall. The highest saturation indices were observed in June 2006, followed by August 2004 and April 2006 (Fig. 6).

Such high saturation states in the plume would favor $CaCO_3$ precipitation. However, substantial $CaCO_3$ formation was not observed in particulate samples collected in intermediate salinity waters (W.-J. Cai unpubl.). The biologically induced pattern of carbonate oversaturation and the associated influence of the Mississippi River and other large river plumes on carbonate dynamics deserve further study.

NCP and its spatiotemporal variation—In general, the calculated NCP was highest at intermediate salinities and lowest in the low-salinity regions (Fig. 8). NCP rates in subregion 1 ranged from -2.9 to 1.2 g C m^{-2} d^{-1} (Table 3; October 2005 was excluded because of the unusual conditions following the hurricanes). In subregion 2, NCP

Table 3. Parameters for the box model, NCP rate, and net OC production in the Mississippi River plume.

Season	Survey	Subregion	Salinity		DIC (μmol kg^{-1})		NCP rate (g C m^{-2} d^{-1})		OC production (10^9 g C d^{-1})		Average NCP rate (g C m^{-2} d^{-1})		DIN load (10^8 mol d^{-1})*	Potential OC production (10^9 g C d^{-1})	Nutrients removal in plume (%)
			Mean	SD	Mean	SD	Mean	SD	Mean	SD	Mean	SD			
Spring	Apr 2006	1	7.6	0.1	2340	102	−2.86	3.88	1.93	3.47	1.06	1.91	1.48	11.7	16
		2	23.9	0.1	1970	92	7.49	5.13							
		3	29.4	0.2	1990	93	0.43	1.44							
		4	32.8	0.2	1990	93	0.53	1.36							
Summer	Jun 2006	1	7.2	0.1	2441	102	1.17	2.39	6.31	3.38	3.96	1.68	1.17	9.3	68
		2	21.7	0.1	1906	90	9.29	5.40							
		3	29.6	0.2	1913	89	0.96	0.89							
		4	33.6	0.2	1991	92	0.30	0.68							
	Aug 2004	1	9.5	0.1	2344	100	−1.06	3.71	4.92	3.38			0.70	5.6	88
		2	24.6	0.1	1897	90	7.34	4.86							
		3	29.0	0.1	1931	91	0.38	1.03							
		4	32.9	0.2	1957	92	0.41	0.88							
Fall	Sep 2006	1	7.2	0.1	2423	105	−2.20	4.06	1.24	1.37	1.14	1.27	0.26	2.1	59
		2	21.6	0.2	2089	96	3.30	2.54							
		3	30.3	0.2	2015	93	0.70	1.31							
		4	32.5	0.2	2002	93	0.58	2.36							

* USGS data at St. Francisville, Louisiana (USGS Sta. 07373420). Data are from the USGS Web page "Water-Quality Data for the Nation" (http://waterdata.usgs.gov/nwis/qw).

rates ranged from 3.3 to 9.3 g C m^{-2} d^{-1}. In subregions 3 and 4, NCP rates ranged from 0.3 to 1.0 g C m^{-2} d^{-1} (Table 3). This pattern is similar to that reported by Lohrenz et al. (1997, 1999) using ^{14}C-derived estimates of primary production. Similarly, Green et al. (2006) also reported high primary production at intermediate salinities–based analyses using food web models. Low productivity in low-salinity areas can be attributed to low light availability, rapid changes in salinity, strong turbulent mixing, and short water residence times (Lohrenz et al. 1999). As nutrients are transported through the turbid, low-salinity region, they become available to support phytoplankton productivity at the intermediate salinities, where there is a more favorable light environment (Lohrenz et al. 1999). Finally, the rates of primary production decrease offshore as nutrients become depleted (Lohrenz et al. 1999; Lehrter et al. 2009). Our results discussed previously regarding carbonate system parameters are generally consistent with this paradigm of biological production in the plume waters.

Using April 2006 results as representative of spring conditions, the average of June 2006 and August 2004 results as summer, and September 2006 results to represent fall, the estimated average plume NCP rates were 1.1, 4.0, and 1.1 g C m^{-2} d^{-1} in spring, summer, and fall, respectively (Table 3). Our NCP rates (Table 3) support the earlier findings of Cai (2003), who estimated DIC uptake rates of 2–3 g C m^{-2} d^{-1} in the Mississippi River plume during August and September 1998. Seasonal total NCP calculated from the area weights of each subplume region times the area and seasonal duration (3 months) yields 1.8, 5.1 and 1.1 $\times$ 10^{11} g C for the spring, summer and fall, respectively. These seasonal estimates agree well with the food web analysis of Green et al. (2006), who calculated seasonal productions of 1.1, 3.4, and 1.3 $\times$ 10^{11} g C for spring, summer, and fall, respectively.

Our estimates of NCP for the Mississippi River plume are the highest reported among the large river plumes in the world, even higher than the net primary production (NPP) in other river plumes and estuaries (Table 4). For example, NCP rates of 0.9–1.6 g C m^{-2} d^{-1} were reported for the Amazon plume (Ternon et al. 2000), and NPP rates of 1.5 g C m^{-2} d^{-1} were observed in the Changjiang plume in a warm season (Ning et al. 1988). NPP rates in the Zaire plume were at least an order of magnitude lower, ranging from 0.05 to 0.25 g C m^{-2} d^{-1} (Cadée 1978). The much higher NCP rates observed in the Mississippi River plume may be attributable to the higher nutrient (DIN) concentrations in the plume (0–32 μmol kg^{-1} at salinities 20–30) than in the cases for the Amazon and Zaire plumes (0–12 and 0–8 μmol kg^{-1}, respectively; Van Bennekom et al. 1978; DeMaster and Pope 1996; Lohrenz et al. 1999), and lower turbidity than that of the Changjiang and Zaire River plumes (Eisma et al. 1978; Ning et al. 1988; Trefry et al. 1994).

Comparison with bottom-water respiration—It is a general feature of large river plumes that high biological production in the surface is accompanied with a strong net respiration in the stratified subsurface waters (Green et al.

Table 4. Comparison of the productivity, DIN concentration, and total suspended materials (TSM) in the plume among the largest rivers.

River	Freshwater discharge (10^{11} m^3 yr^{-1})	DIN in river (μmol kg^{-1})	DIN in plume (μmol kg^{-1})	TSM in plume (mg kg^{-1})	NCP or NPP in plume (g C m^{-2} d^{-1})	References
Mississippi	5.8	70–200	0–100	1–5	1.0–4.0*	Milliman and Meade 1983; Trefry et al. 1994; Lohrenz et al. 1999; Green et al. 2006; this study
Amazon	63.0	17	0–12	<3	1.2–2.4*	Milliman and Boyle 1975; DeMaster and Pope 1996; Ternon et al. 2000; Cooley and Yager 2006
Changjiang	9.0	80–110	5–100	6	1.5†	Ning et al. 1988; Zhang et al. 2007
Zaire	12.5	5–8	0–8	10–15	0.05–0.25†	Cadée 1978; Eisma et al. 1978; Van Bennekom et al. 1978

* NCP.
† NPP.

2006; Chou et al. 2009*b*; Murrell and Lehrter 2011). Water column and benthic respiration rates on the Louisiana shelf were measured by Dortch et al. (1994) and others (*see* Table 4 of Murrell and Lehrter 2011 for a summary).

Most recently, Murrell and Lehrter (2011) reported comprehensive measurements of sediment and water column oxygen consumption rates from eight cruises between 2003 and 2007 with the June and September 2006 cruises overlapping with this study. Their integrated cruise average pelagic (below-pycnocline portion) and benthic respiration rates range from 46 to 105 mmol O_2 m^{-2} d^{-1} (averaged $\sim$ 66 mmol O_2 m^{-2} d^{-1} in spring and summer), which are equivalent to 0.43–0.96 g C m^{-2} d^{-1} assuming a respiratory quotient of 1.3 (O_2 consumed : CO_2 produced). Their estimated rates are lower than plume NCP rates determined in the present study of 1.1 and 4.0 g C m^{-2} d^{-1} for spring and summer, respectively. The reasons that their respiration rates are somewhat lower than our plume NCP rates are twofold. First, the Murrell and Lehrter (2011) respiration data come from both plume and non-plume areas and the lower end of the rates represent areas receiving less OC flux from the plume. Second, OC flux from the plume is likely dispersed over a larger area than the plume itself; thus, direct comparisons are not particularly meaningful. Lehrter et al. (2009) have shown that although the plume areas are net autotrophic, the non-plume areas are net heterotrophic. Therefore, OC production in the river plume represents the most important driving force for heterotrophy in the subsurface and surrounding environments. In a separate paper, we reported the interplay between subsurface-water respiration-induced CO_2 and ocean acidification (Cai et al. in press).

Comparison of net OC production with riverine nutrient loading—The productivity in the Mississippi River plume is strongly influenced by the timing and magnitude of freshwater and nutrient loading from the Mississippi River (Lohrenz et al. 1997) with a much smaller contribution from the Atchafalaya River. As a comparison, we use USGS nutrient data to make a first-order estimate of the potential OC productivity that could be supported by the riverine nutrient inputs, assuming that the Mississippi River was the primary nutrient source for the study area. We ignored atmospheric nitrogen input, which was estimated to be less than 1% of the river input based on nitrogen deposition rates and plume area (Lawrence et al. 2000). DIN loading from the Mississippi River ranged from 0.26 to 1.48 $\times$ 10^8 mol N d^{-1} during the surveyed seasons (Table 3). Assuming Redfield stoichiometry of C : N = 106 : 16, the potential OC production from this DIN source ranged from 2.1 to 11.7 $\times 10^9$ g C d^{-1} (October 2005 was excluded; Table 3).

From this analysis, we concluded that the net OC production estimated from the nonconservative patterns in DIC and TAlk accounted for $\sim$ 60–90% of the potential OC productivity based on the DIN loading during summer and fall (Table 3). In contrast, during spring, the net OC production estimate was only 16% of the potential OC production based on the DIN loading, which was consistent with previous observation (Lohrenz et al. 1997). The distribution of nutrients reported earlier by Lohrenz et al. (1999) support our observations that nutrient concentrations in intermediate salinity regions were higher in spring than that in summer and fall because of the high nutrient load and the relatively lower uptake by phytoplankton in spring. Lehrter et al. (2009) also found that higher discharge decreased the primary production on the Louisiana shelf. Clearly, in addition to nutrient loading, other environmental factors also affect the productivity in the plume. However, a detailed discussion of the limiting factors of productivity in the Mississippi River plume is beyond the scope of this study.

Finally, we must acknowledge that large uncertainties may be involved in our estimates of NCP rates. Improved temporal resolution of biological and chemical dynamics coupled with more precise characterizations of plume physical properties are needed to better constrain process rates in this large river plume system.

In summary, the Mississippi River plume CO_2 biogeochemistry demonstrates interesting impacts of a high-carbonate and high-nutrient large river on coastal oceans. In this study, both DIC and TAlk in the rivers were higher than or similar to those of seawater in the northern Gulf of Mexico, a characteristic that differs from most of the world's major rivers. At intermediate salinity areas of the plume, DIC removal was consistently observed. Together with pH and DO patterns, the results indicated that OC production was the dominant factor responsible for the nonconservative behavior in these constituents.

The spatial and seasonal patterns of saturation states of $CaCO_3$ were similar to those of pH, and the values were much higher than those of average seawater. This implies that the negative effect of ocean acidification on calcareous organisms is not a serious concern in the surface Mississippi River plume. Instead, intense biological production is the dominant factor that increases pH and saturation index of $CaCO_3$. However, this result should not be viewed as evidence against the impacts of ocean acidification on coastal waters. The export of plume-produced OC to the subsurface water and its degradation into CO_2 there should lead to enhanced acidification and decrease of the $CaCO_3$ saturation state below the surface plume (Feely et al. 2010; Cai et al. in press).

NCP was quantified using a box model combined with information about the CO_2 system properties, plume dimensions, and freshwater residence times for the surface mixed layer. The Mississippi River plume has the highest areal-based NCP rate among the large river plumes in the world. This study is the first quantification of NCP derived from plume-wide carbonate field observations in the Mississippi River plume, and the seasonal patterns of NCP were comparable to other studies of primary productivity in the region.

Our results also demonstrated that most of the nutrient load from the Mississippi River was consumed in the turbidity plume during summer and fall, whereas a relatively small fraction was consumed during spring. This pattern, also consistent with prior studies, can be attributed to short residence times, high turbidity, and lower biological uptake rates during spring relative to summer and fall.

Acknowledgments

The cooperation of the crews and the scientific staff of R/V *Pelican* and Ocean Survey Vessel (OSV) *Bold* are appreciated. Guirong Han measured the dissolved inorganic carbon samples. Zhongyong Gao helped with sample collection during the September 2006 cruise. Roman Stanley measured the dissolved oxygen samples on OSV *Bold* cruises. The October 2005 and April 2006 cruises were supported by the National Aeronautics and Space Administration (NASA) through grants NNS04AB84H and NNG05GD22G, under which X.-H. Guo was a visiting student at the University of Georgia. We thank Arthur C.-T. Chen for discussion. Data synthesis and manuscript preparation were supported by National Science Foundation (NSF) Division of Ocean Sciences (OCE)-0752110 (Cai) and OCE-0752254 (Lohrenz), NASA grant NNX10AU06G (Lohrenz and Cai), and the Natural Science Foundation of China (NSFC) through grant 40928006 (Cai and Dai).

References

Bianchi, T. S., T. Filley, K. Dria, and P. G. Hatcher. 2004. Temporal variability in sources of dissolved organic carbon in the lower Mississippi River. Geochim. Cosmochim. Acta **68:** 959–967, doi:10.1016/j.gca.2003.07.011

Borges, A. V., and N. Gypens. 2010. Carbonate chemistry in the coastal zone responds more strongly to eutrophication than to ocean acidification. Limnol. Oceanogr. **55:** 346–353, doi:10.4319/lo.2010.55.1.0346

Brewer, P. G., G. T. F. Wong, M. P. Bacon, and D. W. Spencer. 1975. An oceanic calcium problem? Earth Planet. Sci. Lett. **26:** 81–87, doi:10.1016/0012-821X(75)90179-X

Cadée, G. C. 1978. Primary production and chlorophyll in the Zaire River estuary and plume. Neth. J. Sea Res. **12:** 368–381, doi:10.1016/0077-7579(78)90040-6

Cai, W.-J. 2003. Riverine inorganic carbon flux and rate of biological uptake in the Mississippi River plume. Geophys. Res. Lett. **30:** 1032, doi:10.1029/2002GL016312

———. 2011. Estuarine and coastal ocean carbon paradox: CO_2 sinks or sites of terrestrial carbon incineration? Annu. Rev. Mar. Sci. **3:** 123–145, doi:10.1146/annurev-marine-120709-142723

———, and others. In press. Acidification of subsurface coastal waters enhanced by eutrophication. Nature Geoscience. doi:10.1038/NGEO1297

———, and S. E. Lohrenz. 2010. Marginal seas—the Mississippi River plume and adjacent margin in the Gulf of Mexico, p. 406–421. *In* K. K. Liu, L. Atkinson, R. Quinones, and L. Talaue-McManus [eds.], Carbon and nutrient fluxes in the continental margins: A global synthesis. Springer.

Chen, C. T. A., and A. V. Borges. 2009. Reconciling opposing views on carbon cycling in the coastal ocean: Continental shelves as sinks and near-shore ecosystems as sources of atmospheric CO_2. Deep-Sea Res. II **56:** 578–590, doi:10.1016/j.dsr2.2009.01.001

Chou, W. C., G. C. Gong, D. D. Sheu, C. C. Hung, and T. F. Tseng. 2009*a*. Surface distributions of carbon chemistry parameters in the East China Sea in summer 2007. J. Geophys. Res. **114:** C07026, doi:10.1029/2008JC005128

———, ———, ———, S. Jan, C. C. Hung, and C. C. Chen. 2009*b*. Reconciling the paradox that the heterotrophic waters of the East China Sea shelf act as a significant CO_2 sink during the summertime: Evidence and implications. Geophys. Res. Lett. **36:** L15607, doi:10.1029/2009GL038475

Cochrane, J. D., and F. J. Kelly. 1986. Low frequency circulation on the Texas-Louisiana continental shelf. J. Geophys. Res. **91:** 645–659, doi:10.1029/JC091iC09p10645

Cooley, S. R., and P. L. Yager. 2006. Physical and biological contributions to the western tropical North Atlantic Ocean carbon sink formed by the Amazon River plume. J. Geophys. Res. **111:** C08018, doi:10.1029/2005JC002954

Dagg, M. J., and others. 2005. Biogeochemical characteristics of the lower Mississippi River, USA, during June 2003. Estuaries **28:** 664–674, doi:10.1007/BF02732905

Degens, E. T., S. Kempe, and J. E. Richey. 1991. Summary: Biogeochemistry of the major world rivers, p. 323–347. *In* E. T. Degens, S. Kempe, and J. E. Richey [eds.], Biogeochemistry of major world rivers (SCOPE 42). John Wiley & Sons.

Del Castillo, C. E., and R. L. Miller. 2008. On the use of ocean color remote sensing to measure the transport of dissolved organic carbon by the Mississippi River Plume. Remote Sens. Environ. **112:** 836–844, doi:10.1016/j.rse.2007.06.015

DeMaster, D. J., and R. H. Pope. 1996. Nutrient dynamics in Amazon shelf waters: Results from AMASSEDS. Cont. Shelf Res. **16:** 263–289, doi:10.1016/0278-4343(95)00008-O

Dickson, A. G. 1990. Standard potential of the reaction AgCl(S)+1/2H_2(G)=Ag(S)+HCl(Aq), and the standard acidity constant of the ion HSO_4^- in synthetic sea water from 273.15K to 318.15K. J. Chem. Thermodyn. **22:** 113–127, doi:10.1016/0021-9614(90)90074-Z

Dinnel, S. P., and W. J. Wiseman. 1986. Fresh water on the Louisiana and Texas shelf. Cont. Shelf Res. **6:** 765–784, doi:10.1016/0278-4343(86)90036-1

Dortch, Q., N. N. Rabalais, R. E. Turner, and G. T. Rowe. 1994. Respiration rates and hypoxia on the Louisiana shelf. Estuaries **17:** 862–872, doi:10.2307/1352754

Duan, S. W., and T. S. Bianchi. 2006. Seasonal changes in the abundance and composition of plant pigments in particulate organic carbon in the lower Mississippi and Pearl Rivers. Estuaries Coasts **29:** 427–442, doi:10.1007/BF02784991

Eisma, D., J. Kalf, and S. J. Van Der Gaast. 1978. Suspended matter in the Zaire estuary and the adjacent Atlantic Ocean. Neth. J. Sea Res. **12:** 382–406, doi:10.1016/0077-7579(78)90041-8

Feely, R. A., C. L. Sabine, J. M. Hernandez-Ayon, D. Ianson, and B. Hales. 2008. Evidence for upwelling of corrosive "acidified" water onto the continental shelf. Science **320:** 1490–1492, doi:10.1126/science.1155676

———, and others. 2010. The combined effects of ocean acidification, mixing, and respiration on pH and carbonate saturation in an urbanized estuary. Estuar. Coast. Shelf Sci. **88:** 442–449, doi:10.1016/j.ecss.2010.05.004

Gardner, W. S., R. Benner, G. Chinleo, J. B. Cotner, B. J. Eadie, J. F. Cavaletto, and M. B. Lansing. 1994. Mineralization of organic material and bacterial dynamics in Mississippi River plume water. Estuaries **17:** 816–828, doi:10.2307/1352750

Green, R. E., T. S. Bianchi, M. J. Dagg, N. D. Walker, and G. A. Breed. 2006. An organic carbon budget for the Mississippi River turbidity plume and plume contributions to air-sea CO_2 fluxes and bottom water hypoxia. Estuaries Coasts **29:** 579–597, doi:10.1007/BF02784284

Hitchcock, G. L., W. J. Wiseman, W. C. Boicourt, A. J. Mariano, N. Walker, T. A. Nelsen, and E. Ryan. 1997. Property fields in an effluent plume of the Mississippi river. J. Mar. Syst. **12:** 109–126, doi:10.1016/S0924-7963(96)00092-9

Kleypas, J. A., R. W. Buddemeier, D. Archer, J. P. Gattuso, C. Langdon, and B. N. Opdyke. 1999. Geochemical consequences of increased atmospheric carbon dioxide on coral reefs. Science **284:** 118–120, doi:10.1126/science.284.5411.118

Lawrence, G. B., D. A. Goolsby, W. A. Battaglin, and G. J. Stensland. 2000. Atmospheric nitrogen in the Mississippi River Basin—emissions, deposition and transport. Sci. Total Environ **248:** 87–99, doi:10.1016/S0048-9697(99)00533-1

Ledwell, J. R., A. J. Watson, and C. S. Law. 1993. Evidence for slow mixing across the pycnocline from an open-ocean tracer-release experiment. Nature **364:** 701–703, doi:10.1038/364701a0

Lehrter, J. C., M. C. Murrell, and J. C. Kurtz. 2009. Interactions between freshwater input, light, and phytoplankton dynamics on the Louisiana continental shelf. Cont. Shelf Res. **29:** 1861–1872, doi:10.1016/j.csr.2009.07.001

Levitus, S. 1982. Climatological atlas of the world ocean. NOAA professional paper 13. U.S. Department of Commerce.

Lewis, E., and D. W. R. Wallace. 1998. Program developed for CO_2 system calculations. ORNL/CDLAC-105. Carbon Dioxide Information Analysis Center, Oak Ridge National Laboratory, U. S. Department of Energy.

Lohrenz, S. E., and W.-J. Cai. 2006. Satellite ocean color assessment of air-sea fluxes of CO_2 in a river-dominated coastal margin. Geophys. Res. Lett. **33:** L01601, doi:10.1029/2005GL023942

———, ———, F. Z. Chen, X. G. Chen, and M. Tuel. 2010. Seasonal variability in air-sea fluxes of CO_2 in a river-influenced coastal margin. J. Geophys. Res. **115:** C10034, doi:10.1029/2009JC005608

———, G. L. Fahnenstiel, D. G. Redalje, G. A. Lang, X. G. Chen, and M. J. Dagg. 1997. Variations in primary production of northern Gulf of Mexico continental shelf waters linked to nutrient inputs from the Mississippi River. Mar. Ecol. Prog. Ser. **155:** 45–54, doi:10.3354/meps155045

———, ———, ———, ———, M. J. Dagg, T. E. Whitledge, and Q. Dortch. 1999. Nutrients, irradiance, and mixing as factors regulating primary production in coastal waters impacted by the Mississippi River plume. Cont. Shelf Res. **19:** 1113–1141, doi:10.1016/S0278-4343(99)00012-6

Millero, F. J. 2005. Chemical oceanography. CRC Press.

———, T. B. Graham, F. Huang, H. Bustos-Serrano, and D. Pierrot. 2006. Dissociation constants of carbonic acid in seawater as a function of salinity and temperature. Mar. Chem. **100:** 80–94, doi:10.1016/j.marchem.2005.12.001

Milliman, J. D., and E. Boyle. 1975. Biological uptake of dissolved silica in the Amazon River estuary. Science **189:** 995–997, doi:10.1126/science.189.4207.995

———, and R. H. Meade. 1983. Worldwide delivery of sediment to the oceans. J. Geol. **91:** 1–21, doi:10.1086/628741

Mucci, A. 1983. The solubility of calcite and aragonite in seawater at various salinities, temperatures, and one atmosphere total pressure. Am. J. Sci. **283:** 780–799, doi:10.2475/ajs.283.7.780

Murrell, M. C., and J. C. Lehrter. 2011. Sediment and lower water column oxygen consumption in the seasonally hypoxia region of the Louisiana continental shelf. Estuaries Coasts, **34:** 912–924, doi:10.1007/s12237-010-9351-9

Ning, X., D. Vaulot, Z. Liu, and Z. Liu. 1988. Standing stock and production of phytoplankton in the estuary of the Changjiang (Yangtze River) and the adjacent East China Sea. Mar. Ecol. Prog. Ser. **49:** 141–150, doi:10.3354/meps049141

Ohlmann, J. C., and P. P. Niiler. 2005. Circulation over the continental shelf in the northern Gulf of Mexico. Prog. Oceanogr. **64:** 45–81, doi:10.1016/j.pocean.2005.02.001

Orr, J. C., and others. 2005. Anthropogenic ocean acidification over the twenty-first century and its impact on calcifying organisms. Nature **437:** 681–686, doi:10.1038/nature04095

Pai, S. C., G. C. Gong, and K. K. Liu. 1993. Determination of dissolved oxygen in seawater by direct spectrophotometry of total iodine. Mar. Chem. **41:** 343–351, doi:10.1016/0304-4203(93)90266-Q

Salisbury, J. E., M. Green, C. Hunt, and J. Campbell. 2008. Coastal acidification by rivers: A new threat to shellfish? EOS Trans. Am. Geophys. Union **89:** 513–528, doi:10.1029/2008EO500001

Smith, S. V., and J. T. Hollibaugh. 1993. Coastal metabolism and the oceanic organic carbon balance. Rev. Geophys. **31:** 75–89, doi:10.1029/92RG02584

Ternon, J. F., C. Oudot, A. Dessier, and D. Diverres. 2000. A seasonal tropical sink for atmospheric CO_2 in the Atlantic Ocean: The role of the Amazon River discharge. Mar. Chem. **68:** 183–201, doi:10.1016/S0304-4203(99)00077-8

Trefry, J. H., S. Metz, T. A. Nelsen, R. P. Trocine, and B. J. Eadie. 1994. Transport of particulate organic carbon by the Mississippi River and its fate in the Gulf of Mexico. Estuaries **17:** 839–849, doi:10.2307/1352752

Van Bennekom, A. J., G. W. Berger, W. Helder, and R. T. P. De Vries. 1978. Nutrient distribution in the Zaire estuary and

river plume. Neth. J. Sea Res. **12:** 296–323, doi:10.1016/0077-7579(78)90033-9

Wanninkhof, R. 1992. Relationship between wind speed and gas exchange over the ocean. J. Geophys. Res. **97:** 7373–7382, doi:10.1029/92JC00188

Weiss, R. F. 1974. Carbon dioxide in water and seawater: The solubility of a non-ideal gas. Mar. Chem. **2:** 203–215, doi:10.1016/0304-4203(74)90015-2

Wiseman, W. J., N. N. Rabalais, R. E. Turner, S. P. Dinnel, and A. Macnaughton. 1997. Seasonal and interannual variability within the Louisiana coastal current: Stratification and hypoxia. J. Mar. Syst. **12:** 237–248, doi:10.1016/S0924-7963(96)00100-5

Wysocki, L. A., T. S. Bianchi, R. T. Powell, and N. Reuss. 2006. Spatial variability in the coupling of organic carbon, nutrients, and phytoplankton pigments in surface waters and sediments of the Mississippi River plume. Estuar. Coast. Shelf Sci. **69:** 47–63, doi:10.1016/j.ecss.2006.03.022

Zhai, W. D., and M. H. Dai. 2009. On the seasonal variation of air-sea CO_2 fluxes in the outer Changjiang (Yangtze River) estuary, East China Sea. Mar. Chem. **117:** 2–10, doi:10.1016/j.marchem.2009.02.008

Zhang, J., S. M. Liu, J. L. Ren, Y. Wu, and G. L. Zhang. 2007. Nutrient gradients from the eutrophic Changjiang (Yangtze River) estuary to the oligotrophic Kuroshio waters and re-evaluation of budgets for the East China Sea shelf. Prog. Oceanogr. **74:** 449–478, doi:10.1016/j.pocean.2007.04.019

Associate editor: George W. Kling

Received: 30 September 2010
Amended: 17 August 2011
Accepted: 19 September 2011